Applied Energy 390 (2025) 125767

Contents lists available at ScienceDirect

Applied Energy

journal homepage: www.elsevier.com/locate/apenergy

# Integrating lithium-ion and thermal batteries with heat pumps for enhanced photovoltaic self-consumption

Alicia López-Ceballos *, Carlos del Cañizo, Ignacio Antón, Alejandro Datas *

*Instituto de Energía Solar, Universidad Politécnica de Madrid, Avenida Complutense, 30, 28040, Madrid, Spain*

## HIGHLIGHTS

- Profitability of hybrid PHPS with Li-ion batteries and heat pumps for PV self-use in electrified buildings was assessed.
- PHPS integration boosts PV self-consumption and reduces levelized cost of consumed energy.
- PHPS stores PV peak power and supplies base load energy over extended periods.
- Li-ion batteries deliver high peak power for short durations more effectively.
- Heat pumps enhances hybridization of PHPS with Li-ion batteries rather than replacing PHPS.

## ARTICLE INFO

*Keywords:*
Solar
Photovoltaics
Self-consumption
Thermal energy storage
Power-to-heat-to-power
Thermal batteries
Cogeneration
Combined heat and power
Heat electrification

## ABSTRACT

A promising solution to fully decarbonize the energy consumption of buildings consists of hybridizing solar PV installation with lithium-ion (Li-ion) batteries and heat pumps. However, the high capital cost per unit of energy storage of Li-ion batteries often results in systems with relatively small storage capacities, leading to low self-consumption ratios. Thermal batteries with power generation capacity, such as Power-to-heat-to-power storage (PHPS), leverage the significantly lower cost of thermal energy storage to increase the overall storage capacity of the system. In addition, PHPS systems generate heat as a by-product during the energy conversion, which can be used directly in the building to supply its heating demand.

The goal of this study is to assess the profitability of integrating PHPS systems with heat pumps and Li-ion batteries. A techno-economic analysis, based on a fully-electrified building, demonstrates that the hybridization of PHPS and Li-ion batteries yields the lowest levelized cost of consumed energy, regardless of the coefficient of performance (COP) of the heat pump. This hybrid configuration takes advantage of the lower cost of the energy subsystem of PHPS, which is mostly used for baseload power generation (long duration discharge), and the higher efficiency and lower cost of power capacity of Li-ion batteries, which are optimized for peak power generation (short-duration discharge). Under the assumptions of this study, hybrid solution reduces the levelized cost of consumed energy by 7 % compared to a system relying solely on Li-ion batteries, while simultaneously increasing PV self-consumption by up to 20 %.

## 1. Introduction

Reaching net zero green-house gas emissions by 2050 is imperative to limit the increase of the global mean temperature up to 1.5 °C, compared to the pre-industrial period [1]. Despite intermittent renewable energy sources like solar or wind play a very important role in the decarbonization, mismatch between demand and generation prevents them from scoping a large share in the world-wide energy production. In this regard, several studies have concluded that complementary solutions such as sector-coupling (e.g., through electrification) and energy storage will be necessary to balance this mismatch and fully decarbonize the energy system [2].

Decarbonizing the heating sector is particularly relevant to achieve the climatic goals. For instance, in Europe heat represents 50 % of the energy demand [3], and more than 70 % of the heat is still covered by burning fossil fuels [3]. Heat consumption in buildings is particularly relevant as it accounts for 40 % of the global heating and cooling demand [3]. In this context, heat pumps (HPs) are considered the main enabler of heating electrification. HPs currently cover only 7 % of the

* Corresponding authors.
*E-mail addresses:* a.l.ceballos@upm.es (A. López-Ceballos), a.datas@upm.es (A. Datas).

https://doi.org/10.1016/j.apenergy.2025.125767
Received 12 January 2024; Received in revised form 12 February 2025; Accepted 17 March 2025
Available online 9 April 2025

**Nomenclature**

*Glossary*

| Meaning | |
|---|---|
| CCHP | Combined cooling, heat and power |
| COP | Coefficient of performance |
| CPE | Cost per energy capacity |
| $CPP_{HP}$ | Cost per electrical power capacity of the heat pump |
| $CPP_{out}$ | Cost per output power capacity |
| DHW | Domestic hot water |
| H2P | Heat to power |
| HP | Heat pump |
| HTES | Hot temperature energy storage |
| HWS | Hot water storage |
| L-system | Configuration including only a Li-ion battery |
| LP-system | Configuration including a Li-ion battery and a PHPS system |
| LCOE | Levelized cost of energy |
| LHTPV | Latent heat thermophotovoltaic |
| Li-ion | Lithium ion |
| LTES | Low-temperature energy storage |
| P2H | Power to heat |
| PHPS | Power-to-heat-to-power storage |
| PV | Photovoltaic |
| RTE | Round-trip conversion efficiency |
| SH | Space heating |
| SOC | State of charge |
| TPV | Thermo-photovoltaic |

heating consumption in European buildings [3] and are mainly located in cold climates due to the existing trade-off between high capital investment and operational cost [4,5]. The International Energy Agency states that it will be necessary to install 600 million HPs by 2030 to cover 20 % of the global heating consumption in buildings to be in line with the Zero Emission Scenario [6]. The main problem of electrifying the heating of buildings is the increase and change in the electricity demand profile, as well as its higher dependence on weather conditions [7,8]. As a result, several studies have warned on possible transmission lines overload, pointing at the need of high investments to upgrade the grid infrastructure [3,7,9–11]. To mitigate this issue, some studies propose to partially electrify the space heating sector hybridizing highly-efficient HPs with boilers powered by fossil fuels [11].

An alternative solution to fully electrify buildings consists of developing decentralized photovoltaic (PV) installations for self-consumption with energy storage and heat pumps [12,13]. The number of PV installations for self-consumption is already experiencing a drastic increase [14]. Only in Europe, 20 % of the new PV capacity installed in 2022 was used for residential and industrial/commercial self-consumption [15]. However, uncertainties remain regarding the best energy storage system. Some studies estimated the cost per energy capacity (CPE) for stationary Lithium-ion (Li-ion) batteries could reach values below 100 $/kWh [16–18]. However, current costs range from 200 to 400 €/kWh [19,20], and are subjected to geopolitical issues regarding lithium and other materials' supply that may jeopardize the achievement of low cost in the future. The high CPE of Li-ion batteries result in optimal systems with a relatively small storage capacity favouring its use for short duration purposes. Thus, some studies have assessed hybridizing Li-ion batteries with a cheaper but less efficient energy storage technology (e.g., Redox Flow Batteries) to enhance profitability [19,21]. In this hybrid solution, Li-ion battery enabled reducing the peak of the grid demand by contrast to the cheaper battery which mainly covered the base load [19,21].

Thermal batteries with power generation capacity, or power-to-heat-to-power storage (PHPS) [22–27] are a cheap storage alternative. PHPS stores electricity as thermal energy, typically at very high temperatures (>1000 °C) and converts it back into electricity on demand. The electric-to-electric round-trip conversion efficiency (RTE) of PHPS systems using resistive heating is generally below 50 %. Despite this relatively low RTE, the technology is economically competitive due to its very low CPE (in the range of a few 10's of €/kWh [23,25,26,28]), as well as its ability of dispatching both heat and electricity on demand. Furthermore, the overall efficiency PHPS' can be enhanced by harnessing the waste heat produced during the heat to power (H2P) conversion, either by direct consumption or by storing it for later use. However, the cost per output power capacity ($CPP_{out}$) of the H2P converter is generally high (several 100's €/$kW_{el}$ [26,28,29]). Consequently, optimal system designs typically shift towards large energy-to-(output) power ratios, corresponding to long discharge durations.

PHPS technologies encompass a variety of system designs, each achieving different levels of technological readiness. Most advanced projects [30–34] predominantly employ conventional thermodynamic cycles to produce electricity, like Brayton, Stirling or Rankine which efficiency can go up to 40 % [35]. In contrast, more innovative systems use solid-state thermophotovoltaic (TPV) generators [22,26,27], which have already reported up to 44 % efficiencies [36] and represent a promising avenue for future development.

Hybridizing Li-ion batteries with PHPS could capitalize on their complementarity characteristics, enabling them to meet both peak and base load demand, while utilizing the waste heat generated by PHPS as a valuable by-product. Such a hybrid system could significantly enhance PV self-consumption, thereby reducing reliance on grid electricity. In a previous work [23] we assessed the integration of PHPS with solar PV and air conditioner to achieve dispatchable trigeneration (combined cooling, heat and power or CCHP) in a dwelling equipped with a gas boiler and grid electricity as backup systems. The proposed solution demonstrated the potential to achieve over 70 % savings in electricity demand at reasonable payback periods (<15 y). Similarly, Violidakis et al. [37] investigated the performance of a PHPS system when implemented in a dwelling, concluding that the total electricity and heating demand could be reduced by 20 %. More recently, we explored the application of a specific PHPS technology, a latent heat thermophotovoltaic (LHTPV) battery, in conjunction with solar PV and electric boilers, to fully electrify the energy demand of a building [22]. Our findings indicated that, in this configuration, LHTPV systems could achieve levelized costs lower than those of Li-ion batteries. However, to the best of the authors' knowledge, no study has yet assessed the potential advantages or disadvantages of hybridizing Li-ion battery and PHPS.

Therefore, this article analyses the levelized cost of energy reduction when introducing PHPS in a PV installation with Li-ion battery for self-consumption. The study focuses on a fully electrified dwelling in Madrid that uses either heat pumps or electric boilers for heat production. The results of this analysis will establish the techno-economic targets for PHPS technology developers within the scope of this application. This article aims to assess the following questions:

- Does the hybridization of PHPS with Li-ion batteries reach the lowest Levelized Cost of Energy?
- How does the cost of energy and discharge power of PHPS impact on its economic feasibility? How does the heat pump efficiency and its cost impact on its economic feasibility?
- What are the optimal capacities of PHPS and Li-ion batteries used when hybridized as a function of the analysed parameters?

## 2. System description and methodology

Fig. 1 depicts the two configurations compared within the study: Li-ion battery configuration ("L" system); and the hybrid configuration, which includes both PHPS and Li-ion ("LP" system). In all cases, both heat and electricity demand are covered using electricity from the grid or generated by the PV installation. Surplus of PV generation is stored either in the batteries (Li-ion and PHPS) or in the low temperature thermal energy storage (LTES) system. The LTES system is comprised of a power to heat (P2H) converter and a hot water storage (HWS) tank. In this case, the P2H converter can be an electric heater or a heat pump. The difference lies in the coefficient of performance (COP) defined as the ratio of thermal output power to the electrical input power ($P_{th}/P_{el}$), being COP = 1 for the electric heater, and COP>1 for the heat pump. In the configuration with the heat pump the P2H converter also includes an electric heater (COP = 1) that is used as a back-up when the heat pump maximum capacity is reached. The PHPS system comprises both P2H and H2P converters along with a high temperature energy storage unit (HTES). In this case, a resistive heater (i.e., a furnace) is considered for the P2H converter, being the use of a high temperature heat pump out of the scope of this study. The H2P conversion is accomplished using a heat engine (Brayton, Stirling, Rankine, Thermophotovoltaics, etc.) with a certain discharge efficiency at the operating temperature of the PHPS (>1000 °C). Additionally, the HTES consists of the energy storage material and the insulation layers, which has associated certain self-discharge losses. Finally, the Li-ion battery is composed of an AC/DC converter and the Li-ion battery cells.

The system performance is modelled following an energy decision making tree (illustrated in a simplified scheme in Appendix B). This tree determines the priority order of the energy flows within the system to meet the building's energy demand. Decision-making process for the energy flows remain constant over time and does not incorporate forecasting of electricity cost, energy demand, or PV generation forecasting. The input electricity to the system is used as follows: (1) cover the electricity demand, (2) cover the heating demand, which includes space heating (SH) and domestic hot water (DWH); (3) or charge the energy storage units. The priorities of the energy use are summarized for the LP-system configuration in Table 1 (applies also for the L-system configuration removing the PHPS): (1) Electricity demand is prioritized to be met by PV generation, followed by the PHPS system, and finally by the Li-ion battery; (2) Heating demand is preferentially covered by the LTES, then by PV, PHPS and finally Li-ion; (3) When there is a surplus of PV generation, this is preferably used to charge the Li-ion battery, then the PHPS, and finally the LTES. Any remaining excess PV generation is

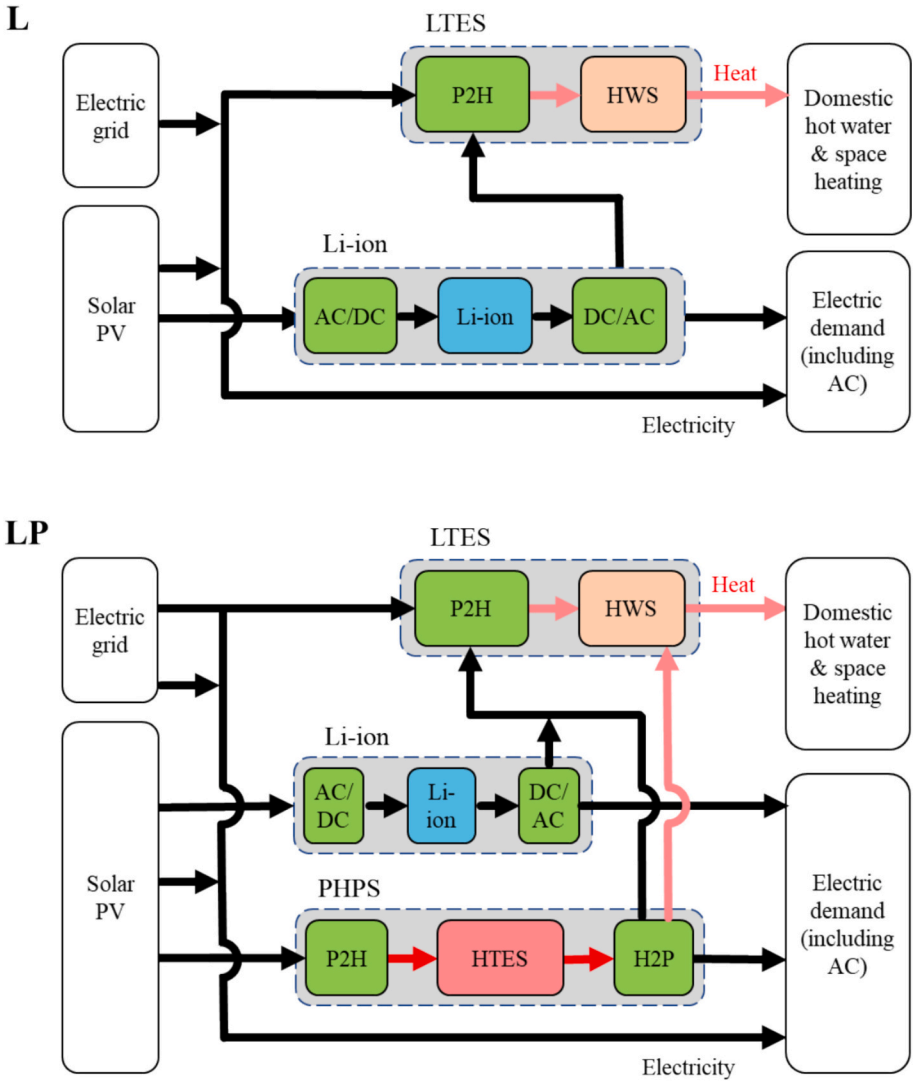


**Fig. 1.** The two system configurations assessed in this work that use only Li-ion battery (case L) or Li-ion hybridized with PHPS (case LP). Black lines represent the flow of electricity, whereas red lines represent the flow of heat. (For interpretation of the references to colour in this figure legend, the reader is referred to the web version of this article.)

**Table 1**
Energy flow priority order.

| Electricity demand | Heat demand | Storage of surplus generation |
|---|---|---|
| 1. PV | 1. Heat from LTES | 1. Li-ion |
| 2. PHPS | 2. Electricity from PV | 2. PHPS |
| 3. Li-ion | 3. Electricity from PHPS | 3. LTES |
| 4. Grid | 4. Electricity from Li-ion | |
| | 5. Electricity from Grid | |

injected into the grid without remuneration.

Li-ion battery is charged first due to its high CPE and superior conversion efficiency, making the energy stored in it more valuable compared to that stored in the PHPS system. As previously mentioned, Li-ion batteries' optimum designs are a small energy capacity and high output power, making them well-suited for covering high peak power demands. In contrast, PHPS is characterized by a high $CPP_{out}$ and low CPE resulting in large energy storage capacities but relatively low output power. This makes PHPS more adequate for base-load operations. Therefore, PHPS is discharged first at low output power to reserve Li-ion when peak demand occurs. In other words, Li-ion battery is discharged only when the PHPS is fully discharged or when the power demand exceeds the maximum output power capacity of PHPS (which is typically low). This approach leverages the low CPP of Li-ion battery and the low CPE of PHPS. While the energy flow priority order outlined in Table 1 influences on the optimal sizing of the components, an in-depth analysis of the best existing (dis)charging strategies is out of the scope of this study.

The system is simulated using hourly resolution data, and the energy flows are determined at every time step for one year based on the State of charge (SOC) of the different storage systems, the PV generation, and the energy demand (both heat and electricity). The hourly PV generation and the residential building energy demand for a site in Madrid are simulated in PVSyst® and EnergyPlus®, respectively, like in our previous work [23]. PV generation for two installation examples are depicted in panels c and d in Fig. A2. Electricity and heating demand are illustrated in panels a and b respectively, in Fig. A2.

The model described above is used to calculate the levelized cost of energy (LCOE) which is given by [38]:

$$LCOE = \frac{CAPEX + \sum_{t=1}^{T} \frac{OPEX(t)}{(1+WACC_{nom})^t}}{\sum_{t=1}^{T} \frac{E_{electr}(t)+E_{heat}(t)}{(1+WACC_{real})^t}} \quad (1)$$

where $CAPEX$ (€) is the initial Capital Expenditure (see Eq. S.1), $OPEX(t)$ (€/year) is the yearly Operational Expenditure (see Eq. S.2), $T$ is the lifetime of the installation (in years) and $E_{electr}(t)$ and $E_{heat}(t)$ (kWh) are the yearly electricity and heat demand, respectively. Finally, $WACC_{nom}$ and $WACC_{real}$ are the Nominal and Real Weighted Average Capital Cost, respectively. $WACC$ in this equation refers to the discount rate of the investment. It is worth noticing that the LCOE defined above refers to the total energy demand (heat and electricity) rather than the total electricity produced by the installation following the same definition shown in [22,23]. Therefore, LCOE is considered as the total operational and capital cost of the installation, normalized to the energy demand in order to compare among different configurations. The LCOE is calculated from 1-year generation and demand data, assuming every year performs equally. The reader might refer to the Appendix A for further details in the calculations.

The sizing of the components in the system is designed to minimize the LCOE. To that end, the Nelder-Mead simplex algorithm is used [39]. This algorithm optimizes different variables to minimize a selected key figure (the LCOE in our case). The algorithm is employed with a set of initial seed values to mitigate the risk of local minima. The optimized parameters are indicated in Table 2 (tagged as 'Optimized'), along with a set of techno-economic parameters needed to calculate the LCOE. The optimized variables are the sizing of the main components in the system: the electrical energy and power storage capacities (PHPS and Li-ion batteries); PV power capacity; LTES energy capacity; and if applicable, the HP electric power capacity. A maximum limit has been set, as indicated in the table, to avoid unrealistic components' sizes for a residential installation (i.e., PV power and LTES energy capacities). Depending on the assumptions, optimum solutions of the LP-system may encompass a combination of both batteries (i.e., PHPS and Li-ion) or only one of them.

All the techno-economic parameters of the components described above are indicated in Table 2. The cost of each component is detached into energy and power subsystems. The CPE and the $CPP_{PHPS\text{-}out}$ of the

**Table 2**
Techno-economic model parameters.[a]

| Component | Parameter | Value |
|---|---|---|
| PV installation | Cost per power capacity | 800 €/kW [42] |
| | Nominal PV power installed | **Optimized** (max. 10 $kW_{el}$) |
| | Cost per energy capacity | 20 €/kWh [43,44] |
| | Cost per electrical power capacity | 10 €/kWh [44] |
| Hot water storage | Energy capacity | **Optimized** (max. 20 $kWh_{th}$) |
| | Electric heater power capacity | Set to cover the peak heating demand ($kW_{el}$) |
| | Electric heater efficiency | 100 % [22] |
| | Self-discharge heat loss ($loss_{tank}$) | 0.1 $W{\cdot}K^{-1}{\cdot}dm^{-3/2}$ [23] [a] |
| | Temperature of storage | 60 °C [22] |
| Li-ion battery | Cost per energy capacity | 255 €/kWh [40] |
| | Energy capacity | **Optimized** (kWh) |
| | Cost per input power capacity | 80 €/$kW_{el}$ [40] |
| | Input power capacity | **Optimized** ($kW_{el}$) |
| | Cost per output power capacity | 0 €/kW [b] |
| | Output power capacity | Equal to the input power capacity |
| | Self-discharge loss | 0%/day [22] |
| | Round-trip efficiency (RTE) | 90 % [22] |
| PHPS | Heat to power efficiency | 40 % [29,45,46] |
| | Power to heat efficiency | 100 % [22] |
| | Cost per energy capacity (CPE) | 30 €/$kWh_{th}$ [23,25,26,28] |
| | Energy capacity | **Optimized** ($kWh_{th}$) |
| | Cost per input power capacity ($CPP_{PHPS\text{-}in}$) | 20 €/$kW_{el}$ [22] |
| | Input power capacity | **Optimized** ($kW_{el}$) |
| | Cost per output power capacity ($CPP_{PHPS\text{-}out}$) | 1000 €/kW [26,28,29] |
| | Output power capacity | **Optimized** ($kW_{el}$) |
| | Self-discharge heat loss | 5 %/day [28,47] |
| Electric heat pump | Cost per electric power capacity | 1000 €/$kW_{el}$ (370 €/$kW_{th}$) [5] |
| | Electric power capacity | **Optimized** ($kW_{el}$) |
| | COP | 2.7 [5] |
| Electric grid | Cost of grid electricity | Variable depending on day and hour. See Fig. A1 |
| | Cost of grid power capacity | Variable depending on hour. See Fig. A1 |
| Other economic variables | Price of electricity injected to the grid | 0 €/kWh |
| | Weighted Average Cost of Capital | 4 % [23] |
| | Inflation | 2 % [23] |
| | Lifetime of all technologies | 25 years [23] |
| Yearly demand | Total energy demand | 20 MWh |
| | Electricity demand | 4 MWh |
| | Heating demand (SH + DHW) | 16 MWh |

[a] This value is based on the standard EN12977–3, according to which, the heat loss coefficient, UA (W/K), is calculated as: $UA = loss_{tank} \cdot \sqrt{V_{tank}}$ [48].
[b] Input power cost of the Li-ion battery is set to 0 €/kW for being the same as the output converter, which is an AC/DC converter.

PHPS are consistent with typical values found in literature on thermal energy storage [23,25,26,28] and high temperature heat engines [26,28,29]. The CPE and CPP for stationary Li-ion battery are 255 €/kWh and 80 €/$kW_{el}$, respectively, corresponding to the forecasted in 2025 [40]. Otherwise indicated, a constant COP of 2.7 is assumed for the heat pump. A COP of 2.5–3 results for an air-to-water HP with a setpoint temperature of 55 °C according to the SH load in Madrid [5]. The cost per electrical power of the HP ($CPP_{HP}$) has been set to 1000 €/$kW_{el}$ (see Fig. 6b) which can be regarded as an optimistic estimate for a small-scale HP [5]. Given the uncertainty regarding PHPS sub-components and for simplification, we assumed that all components in the installation lasts over the PV installation lifetime (25 years). Although Li-ion batteries currently require replacement after 10 years (i.e., the total investment includes the initial unit and 1.5 replacement), we assumed they last the entire installation lifetime of 25 years. This assumption implies that the initial cost ($CPE_{Li\text{-}ion}$ = 255 €/kWh, $CPP_{Li\text{-}ion}$ = 80 €/kW) includes any necessary replacements within the installation's lifetime with equivalent cost of $CPE_{Li\text{-}ion}$ = 130 €/kWh, $CPP_{Li\text{-}ion}$ = 40 €/kW. The electricity tariff agrees with the Spanish regulation for a residential building varying within day of the week and hour for the year 2023 [41]. It should be noted that this assumption could have a significant impact on the results, especially given the current fluctuations in the cost of electricity. No earnings are assumed from selling electricity surpluses to the grid given the uncertainty and variability of this value in the energy market. Despite there should be a trade-off between the cost of the electricity sold and bought from the grid, and the cost of the storages, its impact is out of the scope of this study.

## 3. Results and discussions

The goal of this study is to assess the economic potential of PHPS in a fully electrified building when combined with Li-ion batteries. To that end, the LCOE of the optimal LP-system configuration is compared against the optimal baseline configuration, which relies solely on Li-ion batteries (L-system). This means that the optimum LP-system may result in installations including either both batteries; or only PHPS or Li-ion battery (i.e., ultimately the L-system). This analysis is structured as follows. First, Section 3.1 examines the impact of the cost of PHPS ($CPP_{PHPS\text{-}out}$ and $CPE_{PHPS}$) for two scenarios: (1) a system using just a heat resistance in the P2H unit within the LTES system, and (2) a system incorporating a heat pump with the electric heater as backup for the P2H unit. Subsequently, Section 3.2 evaluates the influence of the heat pump's cost ($CPP_{el\text{-}HP}$) and COP for given PHPS costs. The discussion focuses on identifying the range of values for these key parameters (COP, $CPP_{el\text{-}HP}$, $CPP_{PHPS\text{-}out}$ and $CPE_{PHPS}$) that result in a profitable use of PHPS.

### 3.1. Impact of the cost of PHPS

Fig. 2 shows the reduction in LCOE between the baseline configuration (L-system) and the hybrid configuration (LP-system) as a function of the $CPE_{PHPS}$ (€/kWh) and $CPP_{PHPS\text{-}out}$ (€/$kW_{el}$). Panels a and b show the scenarios using a heat resistance (COP = 1) and a heat pump (COP = 2.7) to cover the heating demand, respectively. Remarkably, the LP-system, which integrates Li-ion batteries with PHPS, proves to be more favourable than the L-system configuration (relying solely on Li-ion batteries), even when incorporating a heat pump, provided that the cost of PHPS is sufficiently low. The maximum tolerable cost of PHPS energy sub-system is around 100 €/kWh (a bit less when using a heat pump), whereas the maximum tolerable cost of the output power subsystem is approximately 2000 €/$kW_{el}$. Therefore, as expected, optimal PHPS system must ensure a low-cost energy storage subsystem, whereas it can tolerate a higher cost of the output power subsystem. Ultimately, this difference between the subsystem costs results in a high optimal energy-to-power capacity ratio, as it will be seen below.

To assess the optimal system sizing based on the cost of the PHPS system, Fig. 3 displays the optimized energy (panels a and b) and power (panels c and d) capacities of the various subcomponents as a function of the cost per output power capacity of the PHPS ($CPP_{out\text{-}PHPS}$). Additionally, Fig. 4 presents the discharge time of PHPS and Li-ion batteries (panels a and b) and the resulting PV self-consumption ratio and the RTE (panels c and d). RTE is defined as the ratio of the total energy demand (combined heat and electricity) and the input energy (ambient heat and electricity, either coming from the PV system or the grid). In other words, RTE only accounts for the energy losses attributed to the utilization of energy storages within the system: energy conversion inefficiencies, unused waste heat (in the H2P conversion), and self-discharge losses. The LCOE is depicted for both scenarios (panels e and f) utilizing a heat resistance (panels a, c and e) and employing a heat pump with COP = 2.7 (panels b, d and f). These parameters are summarized in Table 3 below for $CPE_{PHPS}$ = 30 €/kWh and $CPP_{PHPS}$ = 1000 €/kW.

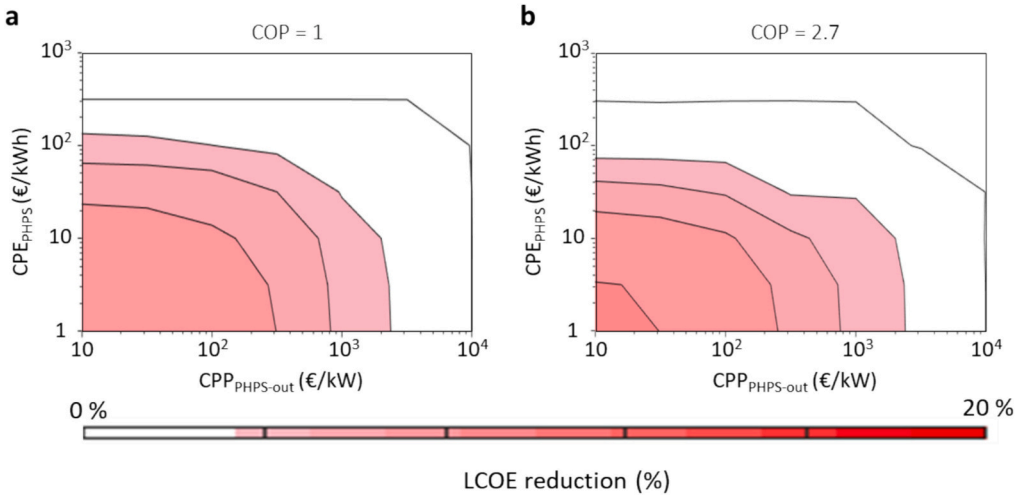


**Fig. 2.** Relative difference in the LCOE between the baseline configuration L-system and the LP-system as a function of the $CPE_{PHPS}$ (€/kWh) and $CPP_{PHPS\text{-}out}$ (€/$kW_{el}$) of the PHPS. Panel a shows the case of a LTES system using only a heat resistance for P2H conversion (COP = 1), whereas panel b shows the case of a LTES system using a heat pump (COP = 2.7). The red regions correspond to situations where the LP-system has lower LCOE than L-system, whereas white regions indicate the optimum LP-system includes only Li-ion battery and removes PHPS. (For interpretation of the references to colour in this figure legend, the reader is referred to the web version of this article.)

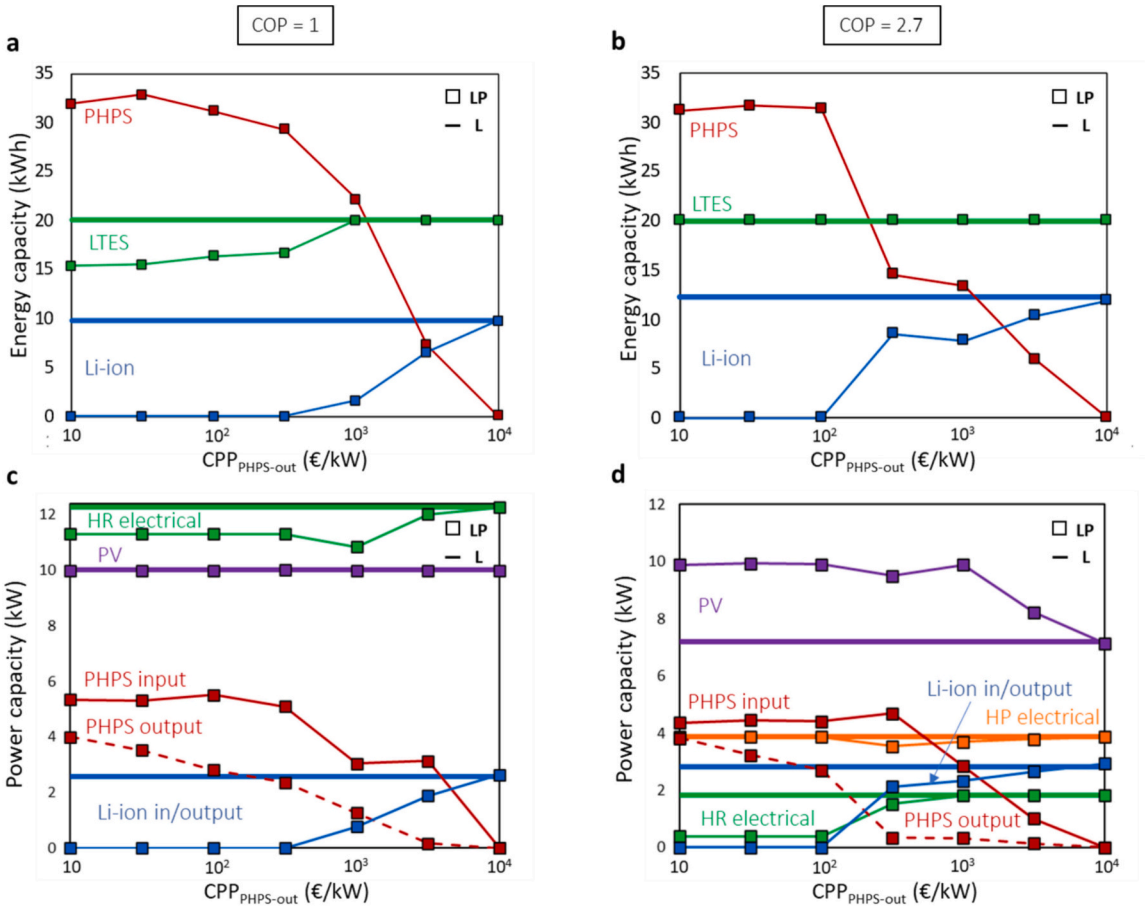


**Fig. 3.** Optimum energy (panels a and b) and power (panels c, and d) capacities of the different components of the two system (LP-system with a square-marker, L-system as a no-marker line) when varying $CPP_{PHPS\text{-}out}$ and fixing $CPE_{PHPS}$ = 30 €/kWh. Results are shown for the case of using an electric boiler (COP = 1, panels a and c) and a heat pump (COP = 2.7, panels b and d). The red and blue lines correspond to the PHPS and Li-ion sizes respectively, the purple solid line is the PV size, the green is the LTES, and the orange one is the HP size (only in panel d). Energy and input power capacities are represented by a solid line, and the PHPS output power capacity is slashed (only for the PHPS since Li-ion has the same input and output power). (For interpretation of the references to colour in this figure legend, the reader is referred to the web version of this article.)

The preference for using a very cheap PHPS over Li-ion batteries is exemplified by the absence of Li-ion batteries in the optimal LP-system when $CPP_{out\text{-}PHPS}$ is low (see panels a and b in Fig. 3). PHPS completely replaces Li-ion by operating as a short-duration energy storage (<5 h panels a and b in Fig. 4). Remarkably, the PV self-consumption ratio of the LP-system is significantly larger than that of the L-system in this case (panels c and d in Fig. 4). This can be attributed to the greater energy storage and input power capacities of PHPS (panels a and c in Fig. 3), which enable the cost-effective storage of surplus solar PV electricity. By contrast, the LP-system exhibits a lower RTE compared to the L-system (panels c and d in Fig. 4), indicating higher overall energy losses within the LP-system. These losses mainly stem from PHPS self-discharge losses and unused waste heat. It is important to note that the RTE does not account for heat pump efficiency, and thus, the presence of a heat pump has minimal impact on this parameter. Despite the L-system achieving a higher RTE, the LP-system can deliver significantly lower LCOE (panels e and f in Fig. 4). This demonstrates that systems with higher overall RTE do not necessarily translate into the most profitable solutions. As $CPP_{PHPS\text{-}out}$ increases, the energy and power capacities of Li-ion batteries rise (panels a, b, c and d in Fig. 3) to compensate for the gradual disappearance of PHPS. Therefore, the optimal LP-system converges towards the L-system configuration, which is rendered as an increase in RTE, at the expense of reduced PV self-consumption due to the diminished PHPS energy capacity. Under these conditions, PHPS is specialized in long-duration applications (>15 h), while Li-ion are optimized for shorter-durations (<5 h) (panels a and b in Fig. 4).

It is noteworthy that utilizing the waste heat produced during the H2P conversion in the PHPS results in a modest reduction of the charging power capacity of the LTES (i.e., the heat resistance -HR- in panels c and d in Fig. 3). Contrary to what could have been expected, the power capacity of the heat pump, which represents a significant portion of the overall installation cost, experiences only a minimal reduction, and it occurs exclusively when both PHPS and Li-ion batteries are integrated into the system (orange line in panel d in Fig. 3, when $CPP_{PHPS\text{-}out}$ = 300–3000 €/kW). Although the introduction of PHPS reduces the equivalent operating hours of the heat pump, the waste heat generated by PHPS and stored in the LTES is insufficient to meet the peak heating demand.

The primary impact of introducing a heat pump is that the optimal solution tends to favour the incorporation of a Li-ion battery, even at relatively low $CPP_{PHPS\text{-}out}$ values (panels b and d in Fig. 3). This presence arises from the superior synergy achieved by combining the highly efficient heat pump with Li-ion batteries, as opposed to relying on the less efficient heat production in the H2P conversion process of PHPS. This higher overall efficiency also leads to a significant reduction in the required PV capacity for the L-system (panel d). However, as stated before, the inclusion of a heat pump with COP = 2.7 has no significant impact on either the PV self-consumption ratio or the overall RTE of the system (panels c and d in Fig. 4). An unexpected consequence of incorporating a heat pump is that the hybrid LP-solution emerges as the optimal choice over a broader range of $CPP_{PHPS\text{-}out}$ values (panels a and b in Fig. 4). In other words, the inclusion of a heat pump does not

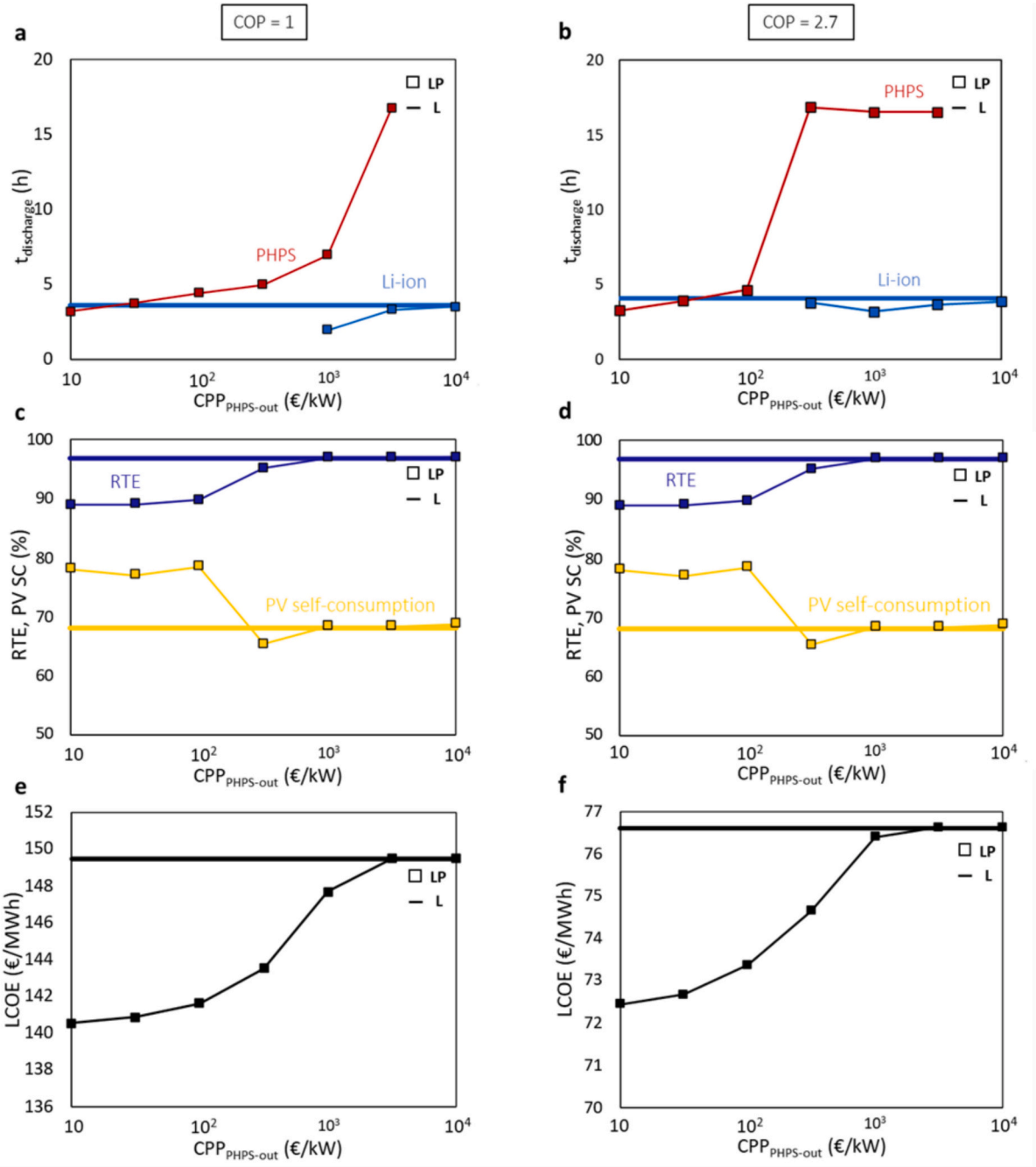


**Fig. 4.** Discharge time is displayed in panels a and b (energy capacity to maximum discharge thermal/chemical power ratio) for the PHPS and Li-ion batteries (red and blue lines respectively). Panels c and d show the overall system RTE (dark blue) and the PV self-consumption (yellow). Panels e and f depict the LCOE in €/MWh. Results are shown for the case of using an electric boiler (COP = 1, panels a, c and e) and a heat pump (COP = 2.7, panels b, d and f). (For interpretation of the references to colour in this figure legend, the reader is referred to the web version of this article.)

entirely replace PHPS in favour of Li-ion batteries but instead promotes the hybridization of PHPS and Li-ion batteries. Importantly, the inclusion of a heat pump also results in a system with a substantially lower LCOE (panels e and f in Fig. 4).

It is also worth noticing that the output power capacity of PHPS is lower than the input PHPS power capacity (panels c and d in Fig. 3). This discrepancy is linked to the differences in the costs of the energy and power sub-systems of the PHPS. Moreover, the energy capacity of PHPS is generally higher than that of Li-ion battery (panels a and b in Fig. 3), which can be attributed to the lower cost of the energy subsystem of PHPS. The combination of the high energy capacity with a high input and low output power capacities of PHPS results in a system that charges faster than it discharges. This design enables PHPS to store high peak power of PV generation and deliver energy base-load power demand over extended periods (>5 h), as depicted in panels a and b in Fig. 4. On the contrary, Li-ion battery is charges and discharges faster, with a maximum rate of less than 5 h (panels a and b in Fig. 4). Therefore, when both technologies coexist in the LP-system configuration, PHPS tackles baseload power demand (long duration discharge times) and Li-ion battery peak power demand (short duration discharge times).

As a reference, the yearly number of cycles per year, calculated as the total yearly input energy divided by the energy capacity of the storage, are 200–220 cycles for PHPS and 260–270 cycles for Li-ion. The difference between charging and discharging processes of the two storage

**Table 3**
Optimal results for the LP and L-cases, $CPE_{PHPS} = 30$ €/kWh and $CPP_{PHPS} = 1000$ €/kW, considering or not the use of a heat pump (COP = 1, COP = 2.7).

| Parameter | COP = 1 | | COP = 2.7 | |
|---|---|---|---|---|
| | LP-case | L-case | LP-case | L-case |
| Minimum LCOE (€/MWh) | 147 | 149 | 76 | 77 |
| Optimal PHPS energy Capacity (kWh) | 22 | - (*) | 13 | - (*) |
| Optimal Li-ion energy Capacity (kWh) | 2 | 10 | 8 | 12 |
| Optimal PV power capacity (kW) | 10 | 10 | 10 | 7 |
| $t_{disch\text{-}PHPS}$ (h) | 7 | – | 16 | – |
| $t_{disch\text{-}li\text{-}ion}$ (h) | 2 | 4 | 3 | 4 |
| PV self-consumption (%) | 79.5 | 68.6 | 68.3 | 68.1 |
| RTE (%) | 91.7 | 97.1 | 96.9 | 96.9 |

(*) Results for the PHPS in the L-case are not included for not being considered in this configuration.

technologies is further illustrated in Fig. 5. This figure depicts the instantaneous input and output electrical power for both PHPS and Li-ion batteries for the LP-system configuration throughout the year. Regardless of the COP value, the PHPS system (panels a and b) is discharged during longer periods than that of Li-ion batteries (panels c and d) all over the year. Li-ion battery is mainly used to provide the peak power electricity demand, and it is predominantly used during the summer period to meet the cooling demand. When including the heat pump (panels b and d), Li-ion battery operates at a higher power level, playing a more prominent role compared to scenarios without a heat pump. In contrast, PHPS is discharged at much lower output power (0.3 $kW_{el}$) but during much longer periods than Li-ion (baseload power generation).

Fig. A2 in Appendix C depict the PV generation (panels c and d) and the electricity imported from the grid (panels e and f) for these two scenarios. Electricity imported from the grid is larger during the winter months, where PV generation is lower. Due to the higher conversion efficiency of the heat pump, the electricity imported is reduced when incorporating the heat pump.

Given the uncertainty of some techno-economic parameters, Fig. A3 and Fig. A4 in Appendix D presents a sensitivity analysis on the variation of Li-ion cost, a parameter expected to fluctuate in the coming years, due to geo-political issues.

### 3.2. Impact of the cost and performance of the heat pump

As seen in the previous section, the hybrid solution (LP-system) combined with a heat pump can provide the lowest LCOE at certain PHPS costs. In contrast, this section is focused on determining the impacts of the COP and cost of the heat pump in the optimal LP-system. Panel a in Fig. 6 includes the difference in LCOE between the L- and LP-systems (positive values representing a LP-system with lower LCOE) as a function of the $CPP_{el\text{-}HP}$ (in €/$kW_{el}$) and the COP of the heat pump. Panels b and c depict the optimal heat pump thermal power capacity for the L and LP-systems respectively, also as a function of the $CPP_{el\text{-}HP}$ (in €/$kW_{el}$) and the COP. Remarkably, results in panel a indicate that the LP-system is consistently preferable over the L-system, regardless of the heat pump COP and cost. The reduction in LCOE is especially pronounced under two scenarios: (1) when the heat pump is very expensive and inefficient (i.e., low COP and high $CPP_{el\text{-}HP}$) or (2) when the heat pump is both inexpensive and highly efficient (i.e., high COP and low $CPP_{el\text{-}HP}$).

The former scenario corresponds to an optimal solution that lacks a heat pump (indicated by the white region in panels b and c), when all the heat is supplied by the backup electric heater. In this case, the LP-system preferentially uses PHPS over Li-ion, taking advantage of the PHPS low cost of energy and the generated waste heat. In the second scenario (high COP and low $CPP_{el\text{-}HP}$), the optimal LP-system takes full advantage of a

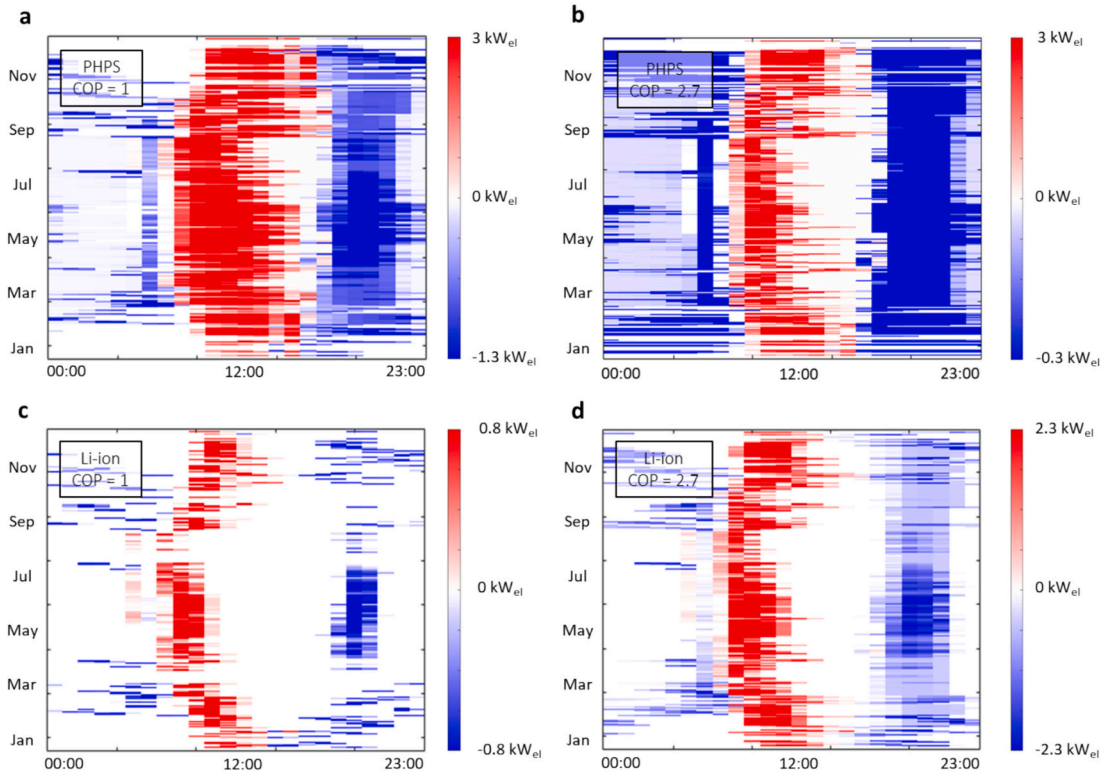


**Fig. 5.** Instant input (positive values, red lines) and output (negative values, blue lines) electrical power. Panels a and b show the PHPS' and panels c and d show Li-ion's results for the LP-system configuration, as a function of the hour of the day (x-axis) and the day of the year (y-axis) when $CPE_{PHPS} = 30$ €/kWh and $CPP_{PHPS\text{-}out} = 1000$ €/$kW_{el}$. Panels a and c, (b and d) show the case without (with) HP. (For interpretation of the references to colour in this figure legend, the reader is referred to the web version of this article.)

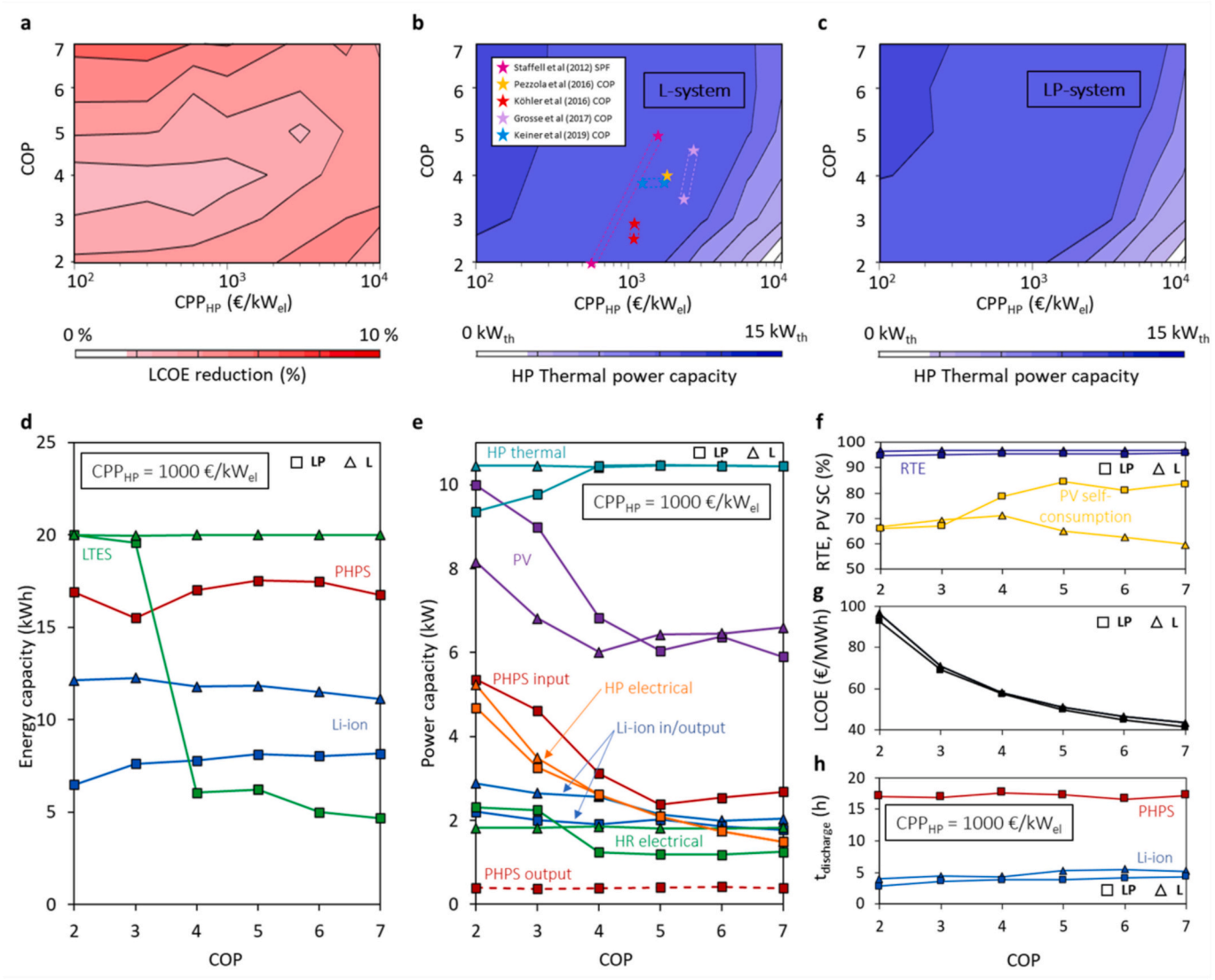


**Fig. 6.** Panel a shows reduction in LCOE between the LP and the L-system configurations as a function of the electrical $CPP_{el\text{-}HP}$ and COP. The case of COP = 1 has not been included for being a special case of the previous study and being the solution independent on the HP cost. Panels b and c show the optimum HP thermal power capacity for the L and LP-system configurations also as a function of the electrical $CPP_{el\text{-}HP}$ and COP. Additionally, panel b plots the COP and $CPP_{el\text{-}HP}$ pair of values from literature are depicted in the fig. [5,49–52]. Panels d and e depict the optimum energy and power capacities (left and right graphs respectively) for the two configurations when varying COP and fixing the heat pump cost to 1000 €/kW$_{el}$. Panel f depicts the RTE (dark blue) and PV self-consumption (yellow), and panel g shows the LCOE (black) for the two systems. Finally, panel h shows the discharge time of the resulting Li-ion and PHPS. L-system and LP-system results are depicted by a triangle and a square respectively. The PHPS sizes are shown by red lines, Li-ion blue, LTES size green, PV purple, and HP thermal capacity in orange. (For interpretation of the references to colour in this figure legend, the reader is referred to the web version of this article.)

cheap and efficient heat pump to downsize most of the system components (panels d and e in Fig. 6), thereby reducing the overall capital investment. Ultimately, the inclusion of such an efficient and low-cost heat pump in a LP-system results in a reduced LCOE (panel g in Fig. 6).

The main advantage of the hybrid LP-system over the L-system lies in its potential to significantly increase PV self-consumption, as illustrated in panel f in Fig. 6. Remarkably, the increment in PV self-consumption of the LP-system compared to the L-system becomes more pronounced at higher COP. As previously discussed, this improvement is attributed to the larger overall storage capacity of the LP-system. The higher PV self-consumption offsets the lower RTE, ultimately resulting in a marginally lower LCOE.

The reduction in LCOE when increasing the COP in both L and LP-systems is partially associated to the capacity reduction in the key components in the installation: PV, heat pump, PHPS, and Li-ion (panel e in Fig. 6). However, it is worth noticing that the heat pump thermal power capacity is barely affected by the COP, especially in the L-system. This is because the thermal power capacity of the heat pump is set to meet the heating demand in the worst-case scenario: wherein there is a peak demand, the LTES is fully discharged, and thus, the heating demand must be entirely satisfied running the heat pump (supported by the heat resistance). The optimal thermal power capacity of the heat pump is reduced only in the scenario where an LP-system with a low COP heat pump is used. This reduction is correlated to an augmented LTES capacity, which capitalizes on the waste heat generated in the PHPS system. In simpler terms: the incorporation of a PHPS system enables a slight reduction in the thermal power capacity of the heat pump.

Finally, panel h in Fig. 6 reveals that the discharge time of both Li-ion and PHPS remains unaffected by variation in the COP. As discussed in the previous section, Li-ion exhibits a discharge duration of approximately 4–5 h, making them well-suited for shorter durations, while PHPS discharges over significantly longer periods (>15 h). The integration of these two storage systems allows Li-ion to specialize in slightly shorter duration applications. This complementary relationship between the two storage systems underscores their essential role in the optimal solution, enabling the system to effectively address both peak and base-load power demands.

## 4. Conclusions

In this study, the economic viability of integrating a PHPS system into a hybridized solution comprising PV, Li-ion batteries and heat pumps in a fully electrified building has been assessed. The proposed hybrid system has been compared to a baseline scenario that includes only a Li-ion battery. A techno-economic model is developed to optimize the sizing of the main components in the system (PV installation, energy and power capacity of the storages, and power capacity of the heat pump) to minimize the levelized cost of the consumed energy. A parametric analysis was conducted to determine the optimal solutions as a function of the cost of the PHPS and the cost and COP of the heat pump. This study is based on energy demand and PV generation data for a residential building located in Madrid. It should be noted that the results presented in this work may vary if applied to different regions or type of building, as factors such as the energy demand profiles, PV generation potential, and the COP for that location are highly context-dependent.

The analysis demonstrates that hybridizing Li-ion batteries with a low-cost PHPS system is generally preferable over a single Li-ion battery installation, irrespective of variations in the costs and COP of the heat pump. The low cost per energy and input power capacity of the PHPS system make it particularly suitable for storing high peak power from PV generation and supplying base-load power demand over longer periods. Contrarily, optimal Li-ion battery specializes in supplying high peak power demand for shorter durations. Therefore, combining the two types of storages in a hybrid system has been identified to be the optimal configuration.

The integration of a PHPS system can increase PV self-consumption by up to 20 % and levelized cost of consumed energy by 7 % compared to a system based solely on Li-ion batteries, despite the slightly lower overall system efficiency. Furthermore, the inclusion of a heat pump enhances the system's efficiency, enabling not only a reduction in electricity demand, but also the downsizing of key system components. Remarkably, the addition of a heat pump does not replace PHPS in favour of Li-ion batteries but instead encourages the hybridization of PHPS and Li-ion batteries, underscoring the complementary roles of these technologies.

## Author contribution

Conceptualization, A.D.; data curation: A.L.C, A.D.; funding acquisition, A.D., C.d.C, I.A.; investigation, A.L.C., A.D.; methodology, A.L.C., A.D.; resources, A.D., I.A.; software: A.L.C., A.D.; visualization: A.L.C., A.D.; writing – original draft: A.L.C., A.D.; writing – review & editing: A. L.C., A.D, C.d.C, I.A.

## CRediT authorship contribution statement

**Alicia López-Ceballos:** Writing – review & editing, Writing – original draft, Visualization, Software, Methodology, Investigation, Data curation. **Carlos del Cañizo:** Writing – review & editing, Funding acquisition. **Ignacio Antón:** Writing – review & editing, Resources, Funding acquisition. **Alejandro Datas:** Writing – review & editing, Writing – original draft, Visualization, Software, Methodology, Investigation, Funding acquisition, Data curation, Conceptualization.

## Declaration of competing interest

The authors declare that they have no known competing financial interests or personal relationships that could have appeared to influence the work reported in this paper.

## Acknowledgements

This work has been funded by the Spanish Ministry of Science and Innovation under grant agreement PID2020-115719RB-C22, from the European Union's Horizon Europe research and Innovation Programme under grant agreement No 101057954, and from the European Union's Horizon 2020 Research and Innovation Programme "SDGine for Healthy People and Cities" in UPM under the Marie Sklodowska-Curie agreement No. 945139. Views and opinions expressed are however those of the author(s) only and do not necessarily reflect those of the European Union or European Innovation Council. Neither the European Union nor the granting authority can be held responsible for them.

## Appendix A. System model and algorithm description

The developed model to assess the technoeconomic study simulates the energy supply (electricity, DHW and SH) of a building, assuming a completely electrified installation. This means that both electricity and heating demand are supplied by electricity sources, in this case the PV installation and the grid. In order to increase PV self-consumption and reduce grid demand, the excess of PV generation is stored in either of the electrical storages (PHPS or Li-ion battery) or the LTES, acting as an electrical and heating back-up respectively. In the following paragraphs only the hybrid configuration is considered, noticing that the PHPS and Li-ion configurations are just a special case of the hybrid one when the other storage is zero. The electrical storages are modelled as containers, independent on how the energy is stored (i.e., thermically, chemically…), that stocks and supplies electricity with certain charging ($\eta_{charge}$) and discharging efficiency ($\eta_{disch}$). These discharging losses (1-$\eta_{disch}$) are considered waste heat at 60 °C if the PHPS is operating.

In each time-step of the simulation period, it is verified separately whether there is electricity or heat demand. This is because LTES can directly supply heat, even if it is a fully electrified system. Hence, the system control prioritizes supplying the electricity demand by the PV generation. If it is not enough, the electrical storages (first PHPS, then Li-ion) provide as much demand as possible, limited by the energy stored and their nominal output power. Finally, the grid covers the rest of the electricity demand. In the case of the PHPS, the heat losses that occur when discharged is either stored in the LTES or directly used to supply the heating load.

If there is heat demand, it is first checked whether the water stored in the LTES is at the setpoint temperature (60 °C). If the temperature is lower, either the PV generation excess, the energy stored in the electrical storages, or the grid, provide, in this order, the electricity required to warm the water up to the setpoint temperature with a power-to-heat (P2H) converter. In case of having a HP as a P2H converter, in addition to the heat resistance, the HP is used up to its maximum power capacity. Once the maximum has been reached, the heat resistance covers the rest of the heat. If there is still PV generation excess after covering both the electricity and heating demand, the system prioritizes charging the electrical storages (first Li-ion, then PHPS), limited by their energy capacity and the maximum input power of the storage. Afterwards, in case of still having excess of PV generation, the system warms up the LTES water up to the setpoint temperature with the P2H converter (first HP, then heat resistance). Finally, the PV electricity surpluses are exported to the grid.

After feeding this model with its inputs: the heating and electricity demand, the PV generation, and the economic and technical assumptions, the simulation is run with hourly resolution for a year following the already explained system control. The resulting yearly data is used to make economic calculations, and in particular, the output of the model which is defined as levelized cost of energy (LCOE). This figure is minimized by an optimization algorithm based on Nelder and Mead for a given sizing of the main components in the system: the PV installation, the energy and power capacity of the electrical storages, the energy and power capacity of the LTES and the HP capacity if applicable.

The LCOE, defined by Eq. 1, is calculated with the capital expenditure *CAPEX* and *OPEX*, shown in Eqs. S.1 and S.2, divided by the total energy demand. This assumption means that LCOE is, in fact, a normalization of the total cost (capital and operational) in order to compare results with and without HP.

$$\begin{aligned} CAPEX = C_{PHPS} + C_{li-ion} + C_{LTES} + C_{PV} + C_{HP} = CPE_{PHPS}\cdot E_{cap-PHPS} + CPP_{in-PHPS}\cdot P_{in-PHPS} + CPP_{out-PHPS}\cdot P_{PHPS} + CPE_{li-ion}\cdot E_{cap-li-ion} + CPP_{in}\cdot P_{in-li-ion} \\ + CPP_{PV}\cdot P_{PV} + CPE_{HW}\cdot E_{cap-LTES} + CPP_{HR}\cdot P_{cap-HR} + CPP_{HP}\cdot P_{HP} \end{aligned} \quad \text{(A1.)}$$

where the *CAPEX* (€) depends on the cost of the electrical storages, $C_{PHPS}$ and $C_{li-ion}$, defined by their cost per energy capacity, $CPE_{PHPS}$ and $CPE_{li-ion}$ (€/kWh), their cost per input and output power capacity, $CPP_{in-PHPS}$, $CPP_{in-li-ion}$and $CPP_{out-PHPS}$ (€/$kW_{el}$) respectively, multiplied by the corresponding storage's sizes: maximum energy capacity, $E_{cap-PHPS}$ and $E_{cap-li-ion}$ (kWh) and maximum input and output power: $P_{in-PHPS}$ $P_{in-li-ion}$, $P_{out-PHPS}$ ($kW_{el}$). The LTES cost, $C_{LTES}$, which is its cost per energy and power capacities, $CPE_{LTES}$ (€/kWh) and $CPP_{HR}$ (€/kW), multiplied by the LTES energy and heat resistance power capacities, $E_{cap-LTES}$ (kWh) and $P_{cap-HR}$ (kW). The PV installation cost, $C_{PV}$, which depends on the cost per power capacity, $CPP_{PV}$ (€/kW), and the total power installed, $P_{nom-PV}$ (kW). And finally, the HP cost $C_{HP}$, calculated multiplying the specific cost $CPP_{HP}$ (€/$kW_{el}$) by the maximum electrical power, $P_{HP}$ ($kW_{el}$)

$$OPEX = W_{grid}\cdot C_{var-grid} + P_{max-grid}\cdot C_{fix-grid} - W_{exp-grid}\cdot C_{exp-var-grid} + P_{PV}\cdot C_{maintenance} \quad \text{(A.2)}$$

The equation above shows that the *OPEX* corresponds to the energy bought from the grid, $W_{grid}$ (kWh), multiplied by the cost in that time period, $C_{var-grid}$ (€/kWh); the maximum contracted power, $P_{max-grid}$(kW) multiplied by the cost per power installed in that period, $C_{fix-grid}$ (€/kW); minus the electricity exported to the grid, $W_{exp-grid}$ (kWh), multiplied by its cost, $C_{exp-var-grid}$ (€/kWh). In addition, the maintenance cost is included depending on its specific power cost, $C_{maintenance}$ (€/kW) and the nominal PV power installed, $P_{PV}$ (kW).

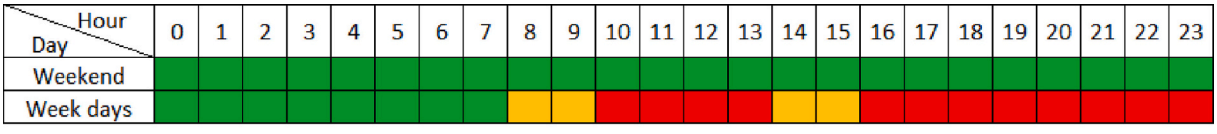


| | Variable cost | Fixed cost |
|---|---|---|
| Low tariff | 0.13 €/kWh | 0.01 €/kW year |
| Mid tariff | 0.17 €/kWh | 0.09 €/kW year |
| High tariff | 0.23 €/kWh | 0.09 €/kW year |

**Fig. A1.** Electricity cost and its schedule for a residential house in Spain which depends on the hour of the day and day of the week. Three periods are distinguished corresponding to low (green), mid (orange) and high (red) tariffs. The variable cost corresponds to the energy cost (€/kWh) whereas the fixed cost means the power cost (€/kW year). (For interpretation of the references to colour in this figure legend, the reader is referred to the web version of this article.)

### A.1. Decision tree

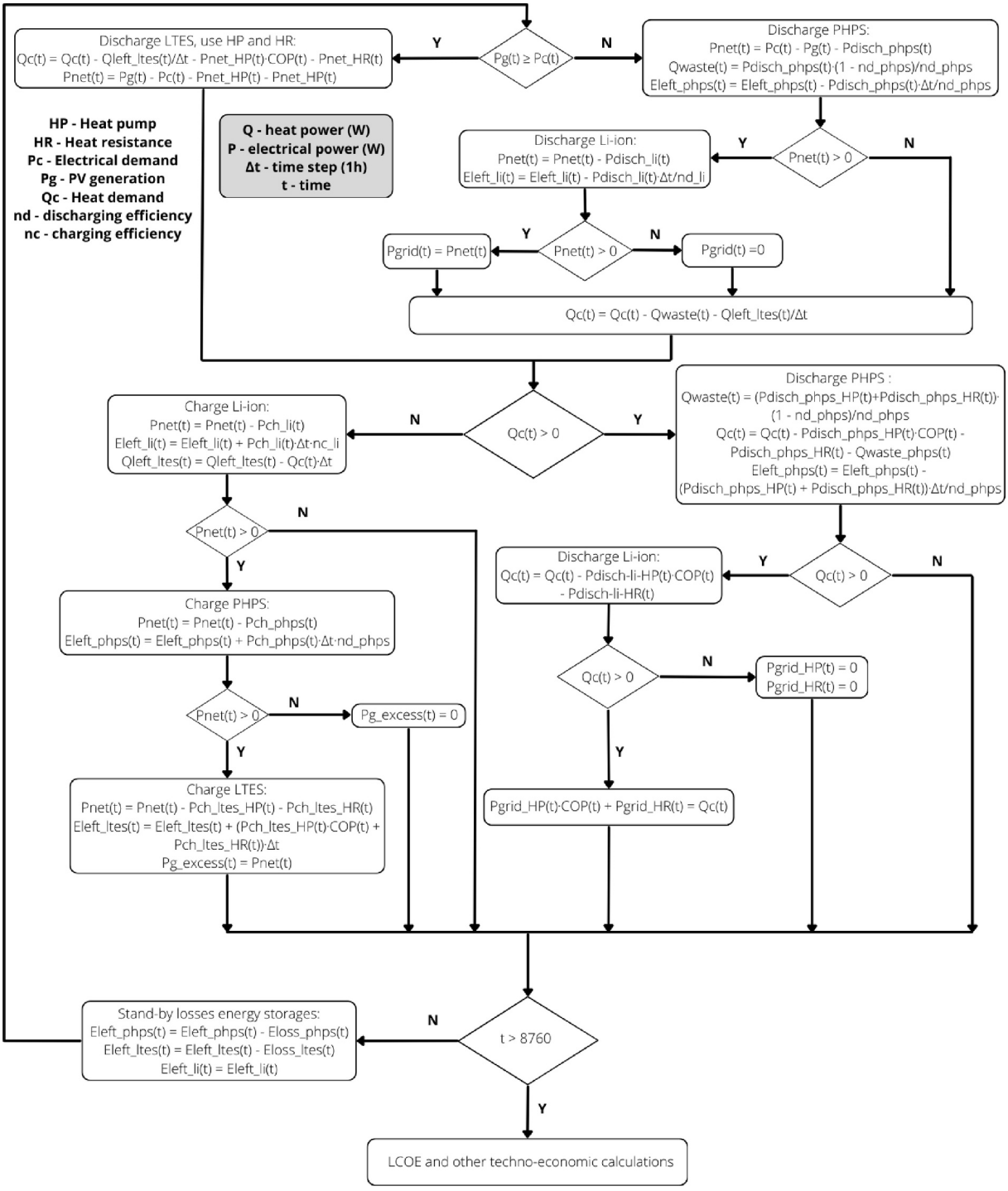

### A.2. Results LP: $CPE_{PHPS} = 30$ €/kWh, $CPP_{PHPS\text{-}out} = 1000$ €/$kW_{el}$

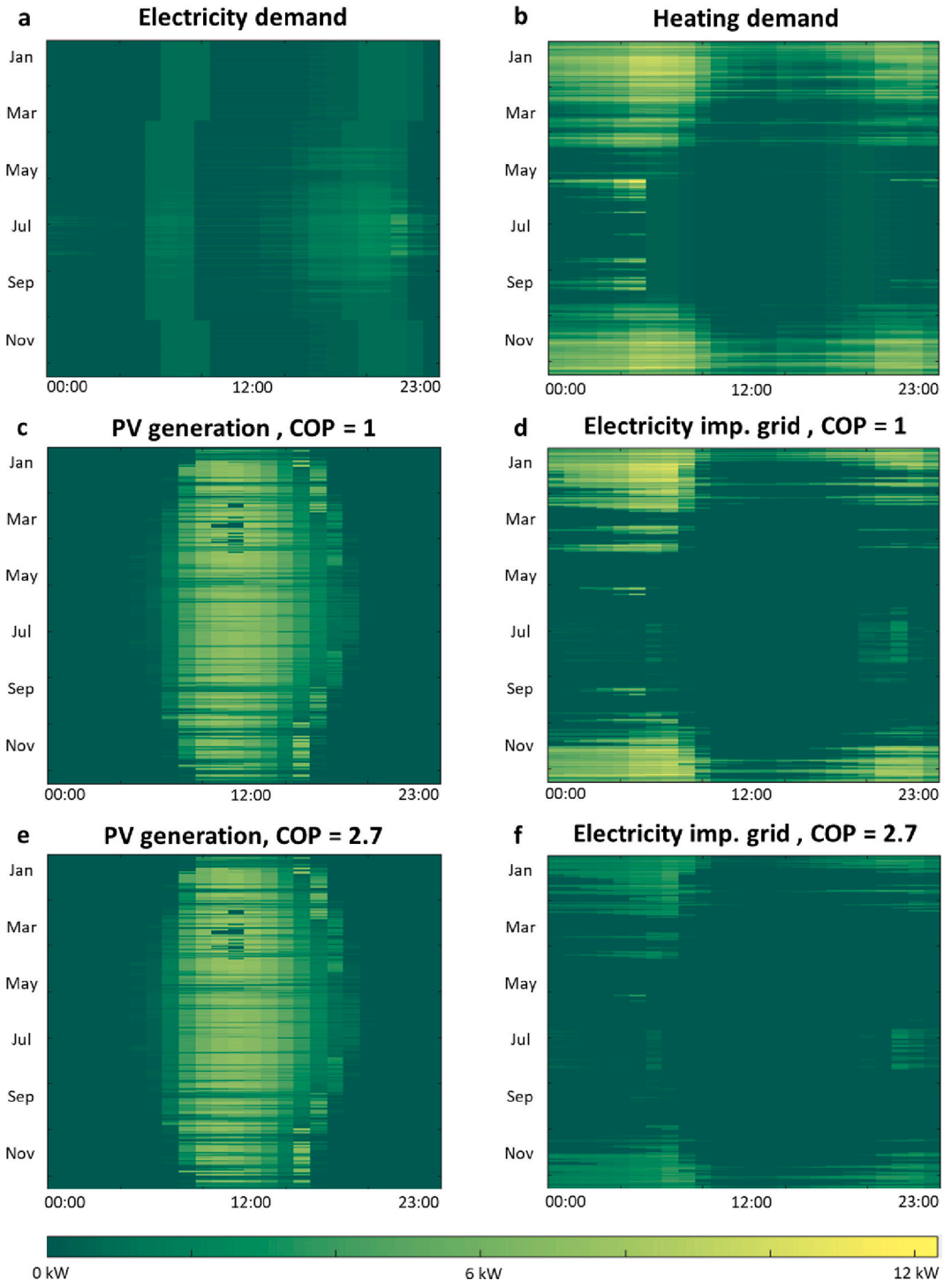


**Fig. A2.** Hourly data for each hour of the day (x-axis) and day of the year (y-axis). Panel a and b show the electricity and demand data of the residential building. The rest of the panels depict results of the PV generation (panels c and e) and electricity imported from the grid (panels d and f) for the LP-configuration assuming $CPE_{PHPS} = 30$ €/kWh and $CPP_{PHPS\text{-}out} = 1000$ €/kW. Panels c and d assume COP = 1 and panels e and f COP = 3.

### A.3. Li-ion cost sensitivity analysis

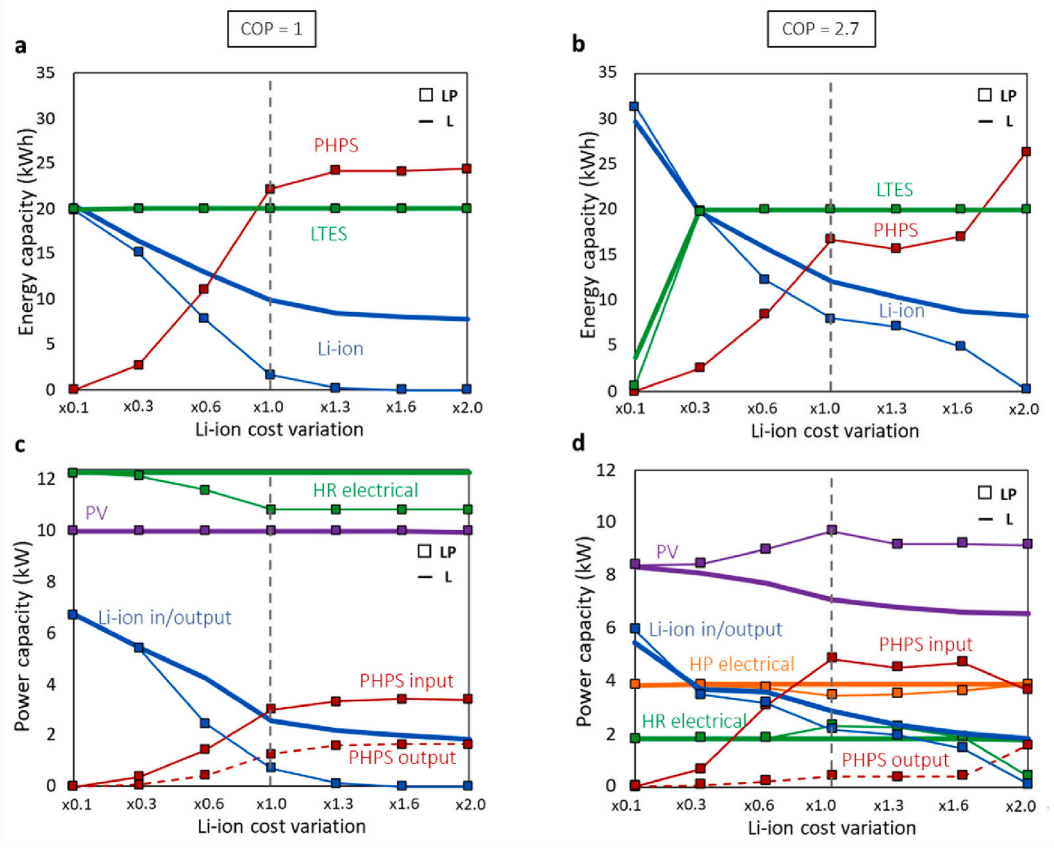


**Fig. A3.** Results varying Li-ion's cost, being the reference $CPE_{Li\text{-}ion} = 255$ €/kWh, $CPP_{Li\text{-}ion\text{-}disch} = 80$ €/kW, when $CPE_{PHPS} = 30$ €/kWh, $CPP_{PHPS\text{-}disch} = 1000$ €/kW. Optimum energy (panels a and b) and power (panels c, and d) capacities of the different components of the two system (LP-system with a square-marker, L-system as a no-marker line) when varying $CPP_{PHPS\text{-}out}$ and fixing $CPE_{PHPS} = 30$ €/kWh. Results are shown for the case of using an electric boiler (COP = 1, panels a and c) and a heat pump (COP = 2.7, panels b and d). The red and blue lines correspond to the PHPS and Li-ion sizes respectively, the purple solid line is the PV size, the green is the LTES, and the orange one is the HP size (only in panel d). Energy and input power capacities are represented by a solid line, and the PHPS output power capacity is slashed (only for the PHPS since Li-ion has the same input and output power). (For interpretation of the references to colour in this figure legend, the reader is referred to the web version of this article.)

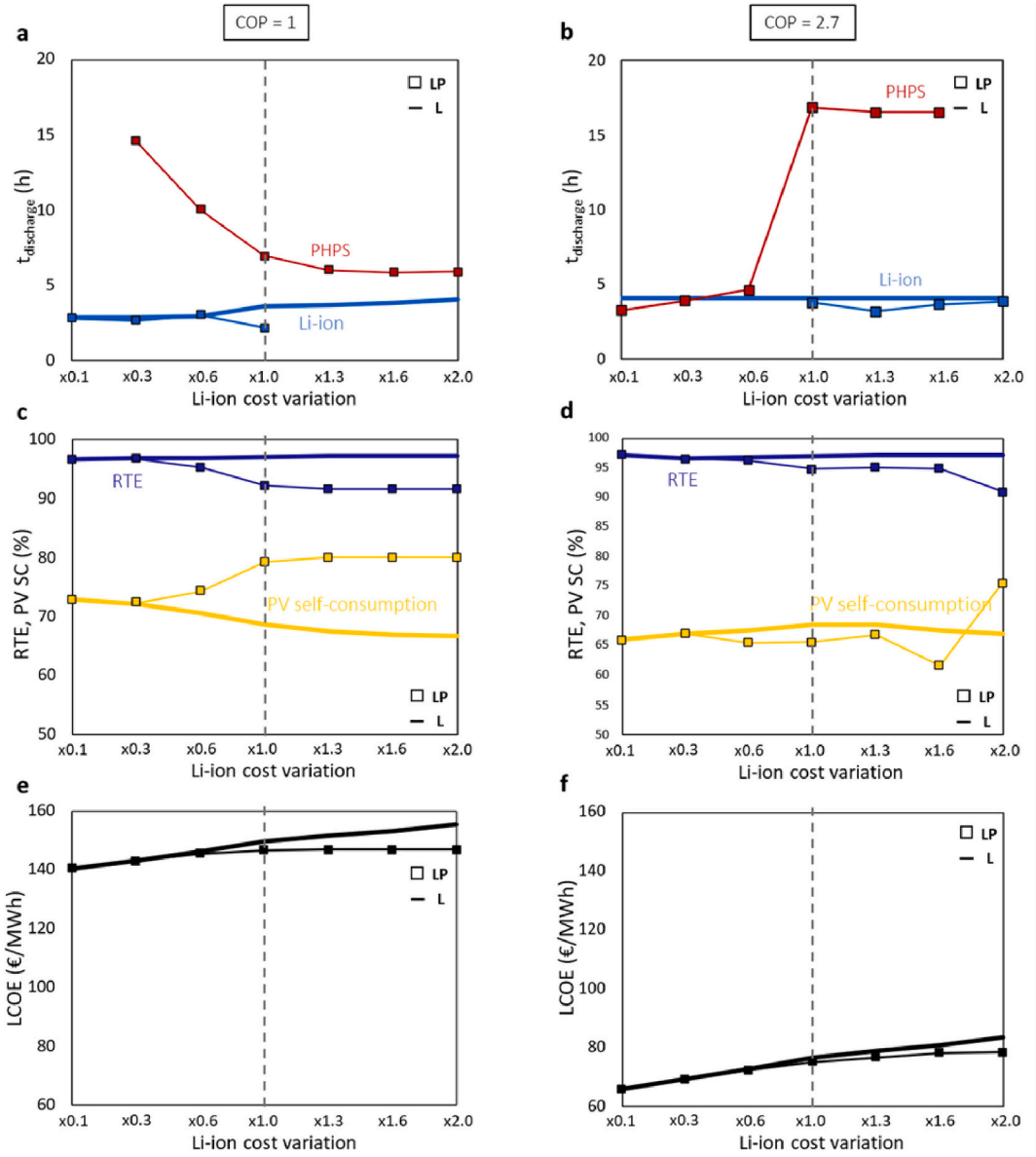


**Fig. A4.** Results varying Li-ion's cost, being the reference $CPE_{Li\text{-}ion}$ = 255 €/kWh, $CPP_{Li\text{-}ion\text{-}disch}$ = 80 €/kW, when $CPE_{PHPS}$ = 30 €/kWh, $CPP_{PHPS\text{-}disch}$ = 1000 €/kW. Discharge time is displayed in panels a and b (energy capacity to maximum discharge thermal/chemical power ratio) for the PHPS and Li-ion batteries (red and blue lines respectively). Panels c and d show the overall system RTE (dark blue) and the PV self-consumption (yellow). Panels e and f depict the LCOE in €/MWh. Results are shown for the case of using an electric boiler (COP = 1, panels a, c and e) and a heat pump (COP = 2.7, panels b, d and f). (For interpretation of the references to colour in this figure legend, the reader is referred to the web version of this article.)

## Data availability

Data will be made available on request.

## References

[1] Rogelj J, et al. "Mitigation pathways compatible with 1.5°C in the context of sustainable development. In: global warming of 1.5°C. An IPCC special report on the impacts of global warming of 1.5°C above pre-industrial levels and related global greenhouse gas emission pathw," IPCC special report global warming of 1.5 °C. 82pp. 2018.

[2] Victoria M, Zhu K, Brown T, Andresen GB, Greiner M. The role of storage technologies throughout the decarbonisation of the sector-coupled European energy system. Energy Convers Manag 2019;vol. 201:111977. no. June, https://doi.org/10.1016/j.enconman.2019.111977.

[3] Kavvadias K, Jiménez-Navarro JP, Thomassen G. Decarbonising the EU heating sector - integration of the power and heating sector. 2019. https://doi.org/10.2760/943257.

[4] Kozarcanin S, Hanna R, Staffell I, Gross R, Andresen GB. Impact of climate change on the cost-optimal mix of decentralised heat pump and gas boiler technologies in Europe. Energy Policy 2020;vol. 140:16–8. https://doi.org/10.1016/j.enpol.2020.111386.

[5] Staffell I, Brett D, Brandon N, Hawkes A. A review of domestic heat pumps. Energy Environ Sci 2012;vol. 5(11):9291–306. https://doi.org/10.1039/c2ee22653g.

[6] IEA, "Heating Analysis.".

[7] Trotter IM, Bolkesjø TF, Jåstad EO, Kirkerud JG. Increased electrification of heating and weather risk in the nordic power system. 2021. p. 1–48 [Online]. Available: http://arxiv.org/abs/2112.02893.

[8] Heinen S, Turner W, Cradden L, McDermott F, O'Malley M. Electrification of residential space heating considering coincidental weather events and building thermal inertia: a system-wide planning analysis. Energy 2017;vol. 127:136–54. https://doi.org/10.1016/j.energy.2017.03.102.

[9] Watson SD, Lomas KJ, Buswell RA. Decarbonising domestic heating: What is the peak GB demand? Energy Policy 2019;vol. 126:533–44. https://doi.org/10.1016/j.enpol.2018.11.001. no. December 2018.

[10] Quiggin D, Buswell R. The implications of heat electrification on national electrical supply-demand balance under published 2050 energy scenarios. Energy 2016;98:253–70. https://doi.org/10.1016/j.energy.2015.11.060.

[11] Waite M, Modi V. Electricity load implications of space heating Decarbonization pathways. Joule 2020;vol. 4(2):376–94. https://doi.org/10.1016/j.joule.2019.11.011.
[12] Battaglia M, Haberl R, Bamberger E, Haller M. Increased self-consumption and grid flexibility of PV and heat pump systems with thermal and electrical storage. Energy Procedia 2017;vol. 135:358–66. https://doi.org/10.1016/j.egypro.2017.09.527.
[13] Franzoi N, Prada A, Verones S, Baggio P. Enhancing PV self-consumption through energy communities in heating-dominated climates. Energies (Basel) 2021;vol. 14 (14):1–17. https://doi.org/10.3390/en14144165.
[14] Uzum B, Onen A, Hasanien HM, Muyeen SM. Rooftop solar pv penetration impacts on distribution network and further growth factors—a comprehensive review. Electro (Switzerland) 2021;vol. 10(1):1–31. https://doi.org/10.3390/electronics10010055.
[15] IEA. Annual solar PV capacity additions by application segment, 2015–2022 – charts – data & statistics - IEA. 2022.
[16] Mongird K, et al. An evaluation of energy storage cost and performance characteristics. Energies (Basel) 2020;vol. 29(13):3307. https://doi.org/10.3390/en13133307.
[17] Schmidt O, Melchior S, Hawkes A, Staffell I. Projecting the future levelized cost of electricity storage technologies. Joule 2019;vol. 3(1):81–100. https://doi.org/10.1016/j.joule.2018.12.008.
[18] Penisa XN, Castro MT, Pascasio JDA, Esparcia EA, Schmidt O, Ocon JD. Projecting the price of lithium-ion NMC battery packs using a multifactor learning curve model. Energies (Basel) 2020;vol. 13(20). https://doi.org/10.3390/en13205276.
[19] Möller M, et al. SimSES: A holistic simulation framework for modeling and analyzing stationary energy storage systems. J Energy Storage 2022;vol. 49: 103743. March 2021, https://doi.org/10.1016/j.est.2021.103743.
[20] Viswanathan V, Mongird K, Franks R. Grid energy storage technology cost and performance assessment. no. August. 2022. p. 1–174. 2022.
[21] Palaniswamy LN, Munzke N, Kupper C, Hiller M. Optimized energy management of a solar and wind equipped student residence with innovative hybrid energy storage and power to heat solutions. Atlantis Press Int BV 2023. https://doi.org/10.2991/978-94-6463-156-2_24.
[22] Datas A, López-Ceballos A, López E, Ramos A, del Cañizo C. Latent heat thermo-photovoltaic batteries. SSRN Electron J 2021:1–26. https://doi.org/10.2139/ssrn.3908778.
[23] Datas A, Ramos A, del Cañizo C. Techno-economic analysis of solar PV power-to-heat-to-power storage and trigeneration in the residential sector. Appl Energy 2019;vol. 256:113935. https://doi.org/10.1016/j.apenergy.2019.113935.
[24] Datas A, Ramos A, Martí A, del Cañizo C, Luque A. Ultra high temperature latent heat energy storage and thermophotovoltaic energy conversion. Energy 2016;vol. 107:542–9. https://doi.org/10.1016/j.energy.2016.04.048.
[25] Okazaki T. Electric thermal energy storage and advantage of rotating heater having synchronous inertia. Renew Energy 2020;vol. 151:563–74. https://doi.org/10.1016/j.renene.2019.11.051.
[26] Amy C, Seyf HR, Steiner MA, Friedman DJ, Henry A. Thermal energy grid storage using multi-junction photovoltaics. Energy Environ Sci 2019;vol. 12(1):334–43. https://doi.org/10.1039/c8ee02341g.
[27] Datas A. Ultra high temperature thermal energy storage for dispatchable power generation. Ref Mod Earth Syst Environ Sci Jan. 2021. https://doi.org/10.1016/B978-0-12-819723-3.00088-3.
[28] Datas A, López-Ceballos A, López E, Ramos A, del Cañizo C. Latent heat thermophotovoltaic batteries. Joule Feb. 2022;vol. 6(2):418–43. https://doi.org/10.1016/J.JOULE.2022.01.010.
[29] Mazzetti A, Gianotti Pret M, Pinarello G, Celotti L, Piskacev M, Cowley A. Heat to electricity conversion systems for moon exploration scenarios: a review of space and ground technologies. Acta Astro 2019;vol. 156:162–86. https://doi.org/10.1016/j.actaastro.2018.09.025.
[30] 1414 Degrees to power abandoned Aurora CSP site with PV and thermal storage. https://www.pv-magazine-australia.com/2019/11/29/1414-degrees-to-power-abandoned-aurora-csp-site-with-pv-and-thermal-storage/.
[31] Gamesa, "Industrial decarbonization using electric thermal energy storage (ETES)," 2020. Accessed: Nov. 20, 2024. [Online]. Available: https://www.siemensgamesa.com/global/en/home/press-releases/20180926-sgre-storage-hamburg-etes.html.
[32] X-company, "Malta energy storage.".
[33] Thermal energy storage. 21; 2022. Accessed: Feb [Online]. Available: https://antoraenergy.com/technology.
[34] Antora energy raises more than $50M to decarbonize heavy industry with renewable heat and power as cheap as fossil fuels. 2022.
[35] Mazzetti A, Gianotti Pret M, Pinarello G, Celotti L, Piskacev M, Cowley A. Heat to electricity conversion systems for moon exploration scenarios: a review of space and ground technologies. Acta Astro 2019;vol. 156:162–86. https://doi.org/10.1016/j.actaastro.2018.09.025.
[36] Roy-Layinde B, Lim J, Arneson C, Forrest SR, Lenert A. High-efficiency air-bridge thermophotovoltaic cells. Joule Jul. 2024;vol. 8:2135–45. https://doi.org/10.1016/j.joule.2024.05.002.
[37] Violidakis M, Zeneli K, Atsonios G, Strotos N Nikolopoulos, Karellas S. Dynamic modelling of an ultra high temperature PCM with combined heat and electricity production for application at residential buildings. Energ Build 2020;vol. 222. https://doi.org/10.1016/j.enbuild.2020.110067.
[38] JRC photovoltaic geographical information system (PVGIS) - European commission. Accessed: May 13. [Online]. Available: https://re.jrc.ec.europa.eu/pvg_tools/es/?lat=&lon=&startyear=&endyear=&raddatabase=&angle=&browser=&outputformat=&userhorizon=&usehorizon=1&js=1&select_database_month=PVGIS-SARAH&mstartyear=2005&mendyear=2005&optrad=1&selectrad=1&mangle=36#MR; 2021.
[39] D'Errico J. Fminsearchbnd, fminsearchcon - file exchange - MATLAB central. Accessed: May 14. [Online]. Available: https://es.mathworks.com/matlabcentral/fileexchange/8277-fminsearchbnd-fminsearchcon; 2021.
[40] Viswanathan V, Mongird K, Franks R, Li X, Sprenkle V. Grid energy storage technology cost and performance assessment. no. August. 2022. p. 151.
[41] Mejores tarifas de luz 2023. ¿Cómo elegir la mejor tarifa de luz?. Accessed: Feb. 28, 2023. [Online]. Available: https://comparadorluz.com/tarifas/luz; 2023.
[42] Victoria M, Zhu K, Zeyen E, Brown T. Costs PyPSA. Accessed: May 19, 2021. [Online]. Available: https://github.com/PyPSA/technology-data/blob/master/outputs/costs_2020.csv; 2020.
[43] Bagheri-Esfeh H, Dehghan MR. Techno-economic design of a solar combisystem in a residential building. J Build Eng Jul. 2023;vol. 71:106591. https://doi.org/10.1016/J.JOBE.2023.106591.
[44] EASE. Thermal hot water storage. Thermal energy storage. Eu Associat Storage Energy 2016:1–2.
[45] Thess A. Thermodynamic efficiency of pumped heat electricity storage. Phys Rev Lett 2013;vol. 111(11):1–5. https://doi.org/10.1103/PhysRevLett.111.110602.
[46] Narayan TC, et al. World record demonstration of > 30% thermophotovoltaic conversion efficiency. In: In 2020 47th IEEE photovoltaic specialists conference (PVSC); 2020. p. 1792–5. https://doi.org/10.1109/pvsc45281.2020.9300768. Calgary.
[47] Voesch W, Wanke R, Rastegar I, Braun W, Kribus A, Mannhart J. High-temperature latent-heat energy storage concept based on thermoelectronic energy conversion. Energ Technol 2017;vol. 5(12):2234–43. https://doi.org/10.1002/ente.201700273.
[48] Thermal solar systems and components [Online]. Available, www.din.de; Jul. 2018.
[49] Keiner D, Ram M, Barbosa LDSNS, Bogdanov D, Breyer C. Cost optimal self-consumption of PV prosumers with stationary batteries, heat pumps, thermal energy storage and electric vehicles across the world up to 2050. Sol Energy 2019; vol. 185:406–23. https://doi.org/10.1016/j.solener.2019.04.081. no. April.
[50] Pezzola L, Danti P, Magnani S. Performance comparison among gas heat pump, electric heat pump and conventional thermal devices in tertiary sector applications. Energy Procedia 2016;vol. 101:416–23. https://doi.org/10.1016/j.egypro.2016.11.053. no. September.
[51] Grosse R, Christopher B, Stefan W, Geyer R, Robbi S. Long term (2050) projections of techno-economic performance of large-scale heating and cooling in the EU. Luxembourg: Publications Office of the European Union; 2017. https://doi.org/10.2760/24422.
[52] Köhler B, Bonato P, Steinbach J, Ragwitz M. Mapping and analyses of the current and future (2020−2030) heating technologies for the year 2012. 2016. https://doi.org/10.13140/RG.2.2.28214.96329.